Improving Penetration in Tumors With Nanoassemblies of Phospholipids and Doxorubicin

Ning Tang, Gangjun Du, Nan Wang, Chunchun Liu, Haiying Hang, Wei Liang

Background Drug delivery and penetration into neoplastic cells distant from tumor vessels is critical for the effectiveness of solid tumor chemotherapy. We hypothesized that 10- to 20-nm nanoassemblies of phospholipids containing doxorubicin would improve the drug's penetration, accumulation, and antitumor activity.

Methods Doxorubicin was incorporated into polyethylene glycol–phosphatidylethanolamine (PEG-PE) block copolymer micelles by a self-assembly procedure to form nanoassemblies of doxorubicin and PEG-PE. In vitro cytotoxicity of micelle-encapsulated doxorubicin (M-Dox) against A549 human non–small-cell lung carcinoma cells was examined using the methylthiazoletetrazolium assay, and confocal microscopy, total internal reflection fluorescence microscopy, and flow cytometry were used to examine intracellular distribution and the cellular uptake mechanism. C57Bl/6 mice (n = 10–40 per group) bearing subcutaneous or pulmonary Lewis lung carcinoma (LLC) tumors were treated with M-Dox or free doxorubicin, and tumor growth, doxorubicin pharmacokinetics, and mortality were compared. Toxicity was analyzed in tumor-free mice. All statistical tests were two-sided.

Results Encapsulation of doxorubicin in PEG-PE micelles increased its internalization by A549 cells into lysosomes and enhanced cytotoxicity. Drug-encapsulated doxorubicin was more effective in inhibiting tumor growth in the subcutaneous LLC tumor model (mean tumor volumes in mice treated with 5 mg/kg M-Dox = 1126 mm^3 and in control mice = 3693 mm^3, difference = 2567 mm^3, 95% confidence interval [CI] = 2190 to 2943 mm^3, $P<.001$) than free doxorubicin (mean tumor volumes in doxorubicin-treated mice = 3021 mm^3 and in control mice = 3693 mm^3, difference = 672 mm^3, 95% CI = 296 to 1049 mm^3, $P = .0332$, Wilcoxon signed rank test). M-Dox treatment prolonged survival in both mouse models and reduced metastases in the pulmonary model; it also reduced toxicity.

Conclusions We have developed a novel PEG-PE–based nanocarrier of doxorubicin that increased cytotoxicity in vitro and enhanced antitumor activity in vivo with low systemic toxicity. This drug packaging technology may provide a new strategy for design of cancer therapies.

J Natl Cancer Inst 2007;99:1004–15

Solid tumors account for more than 85% of cancer mortality. To obtain nutrients for growth and to metastasize, cancer cells in solid tumors must grow around existing vessels or stimulate formation of new blood vessels. These new vessels are abnormal in structure and characterized by leakage, tortuousness, dilation, and a haphazard pattern of interconnection (1–4). Tumor structure and blood flow hinder the treatment of solid tumors (5,6). To reach cancer cells in optimal quantity, a therapeutic agent must pass through an imperfect blood vasculature to the tumor, cross vessel walls into the interstitium, and penetrate multiple layers of solid tumor cells. Recent studies have demonstrated that poor penetration and limited distribution of doxorubicin in solid tumors are the main causes of its inadequacy as a chemotherapeutic agent (7,8).

To address these challenges, different strategies have been investigated. One approach is to reduce tumor interstitial pressure by modulation of vascular endothelial barrier function to improve penetration of chemotherapeutic drug into tumors. This approach could enhance the antitumor activity of chemotherapeutic drugs, without increasing toxicity (9,10). Another strategy is to use nano-sized carriers to deliver a chemotherapeutic drug deeply into the tumor. The three-dimensional penetration of macromolecules into the tumor interstitium from the vascular surface has been

Affiliations of authors: Protein & Peptide Pharmaceutical Laboratory, National Laboratory of Biomacromolecules (NT, GD, WL) and Center for Infection and Immunity (CL, HH), Institute of Biophysics, Chinese Academy of Sciences, Beijing, China; Institute of Materia Medica, Chinese Academy of Medical Sciences, Beijing, China (NW).

Correspondence to: Wei Liang, PhD, Protein & Peptide Pharmaceutical Laboratory, National Laboratory of Biomacromolecules, Institute of Biophysics, Chinese Academy of Sciences, Beijing 100101, China (e-mail: weixx@sun5.ibp.ac.cn) or Haiying Hang, PhD, Center for Infection and Immunity, Institute of Biophysics, Chinese Academy of Sciences, Beijing 100101, China (e-mail: hh91@sun5.ibp.ac.cn).

See "Funding" and "Notes" following "References."

DOI: 10.1093/jnci/djm027

studied using the dorsal skin fold window chamber model with results that indicated that an increase in molecular weight decreases penetration into tumors from the vascular surface but increases retention time. Dextrans with a molecular weight between 40 and 70 kDa (and a diameter of 11.2–14.6 nm) provided the greatest tumor penetration and accumulation (11). Based on these findings, an optimal size of nanocarrier for chemotherapeutic drugs may be designed for treatment of solid tumors. The PEG-PE molecule, which consists of both hydrophilic polyethylene glycol (PEG) and hydrophobic phosphatidylethanolamine (PE) segments, is an amphiphilic copolymer that is ideal for forming micelles. PEG-PE micelles have a low critical micelle concentration and are small (~10–20 nm), both of which are desired features in nanocarriers of drugs (12–14). In this study, we investigated the penetration and accumulation of doxorubicin encapsulated in PEG-PE micelles in tumors and its efficacy in murine cancer models.

CONTEXT AND CAVEATS

Prior knowledge

The inadequate penetration and limited distribution of doxorubicin in tumors reduce its effectiveness as a chemotherapeutic agent. Although various nanocarriers that encapsulate chemotherapeutic agents have shown potential to improve drug delivery to the tumor and reduce systemic toxicity, they also tend to decrease the cytoxicity of the drugs.

Study design

Properties of a drug-loaded nanocarrier and the free drug were compared using in assays of cellular uptake and cytotoxicity and by studying tumor growth and survival in mouse models.

Contribution

This work presents a strategy for micelle encapsulization of doxorubicin that enhances its cytoxicity and accumulation in cells and increases its efficacy in inhibiting tumor growth in vivo.

Implications

Micelle encapsulization of doxorubicin and other drugs may have the potential to improve the effectivness of these agents while reducing side effects.

Limitations

A comprehensive physical and structural characterization of the drug-loaded nanocarrier is needed for a mechanistic understanding of its action.

Materials and Methods

Cell Culture

Human non–small-cell lung carcinoma (A549) cells were purchased from American Type Culture Collection (ATCC; Manassas, VA). Cell culture medium and fetal bovine serum were from Invitrogen (Carlsbad, CA). Culture flasks and dishes were from Corning (Corning, New York, NY). Cells were cultured in RPMI 1640 medium supplemented with 10% heat-inactivated fetal bovine serum, penicillin (100 U/mL), and streptomycin (100 U/mL).

Preparation of Micelles Encapsulating Doxorubicin

Doxorubicin (doxorubicin hydrochloride, provided by HaiZheng Corp, Taizhou, Zhenjiang, China) was dissolved in methanol at room temperature (stoichiometric molar ratio of doxorubicin : triethylamine [Sigma, St Louis, MO] = 1 : 2) and then mixed with PEG-PE (Avanti Polar Lipids, Alabaster, AL) in chloroform (Sigma) at a PEG-PE molar ration of 1 : 2. The organic solvents were removed using a rotary evaporator to form the drug-containing lipid film. To form micelle-encapsulated doxorubicin (M-Dox), the lipid film was hydrated with 10 mM HEPES-buffered saline (HBS, pH 7.4) at 37 °C for 30 minutes. The doxorubicin-loaded micelles were extruded through a membrane of pore size 200 nm. The final concentration of doxorubicin in micelles was 2 mg/mL as determined by high-performance liquid chromatography (HPLC). The degraded products of doxorubicin incorporated in micelles were detected using HPLC after defined periods of storage.

Study of the Physicochemical Properties of Micelle-Encapsulated Doxorubicin

The size and morphology of micelles encapsulating doxorubicin were examined using dynamic light scattering and transmission electron microscopy (TEM). Empty micelles or M-Dox were diluted to a concentration of 1 mg/mL with deionized water. The micelles were stained with 1% uranyl acetate and examined with a JEOL 100 CX electron microscope (JEOL USA, Inc, Peabody, MA). The size of the micelles was determind with a Zetasizer 5000 (Malvern Instruments, Malvern, Worcestershire, U.K.).

To determine the kinetics of doxorubicin release from micelles, 0.5 mL of M-Dox was added to 0.5 mL HBS or fresh mouse serum such that the doxorubicin concentration was 1 mg/mL and the mixture was placed in a dialysis bag (molecular mass cutoff 10 kDa). The dialysis bags were incubated in 150 mL of either phosphate buffer (pH 7.0) or acetate buffer (pH 5.0) at 37 °C with gentle shaking, and aliquots of incubation medium were removed from the incubation medium at predetermined time points. The released drug was quantified fluorimetrically using reverse-phase HPLC with a C18 column, with acetic acid, methanol, and 10 mM $NH_4H_2PO_4$ (0.5:95:60, vol/vol/vol, pH 3.2) as the eluant solution.

Analysis of Cytotoxicity

A549 cells were plated at a density of 5×10^3 cells per well in 100 μL RPMI 1640 medium in 96-well plates and grown for 24 hours. The cells were then exposed to a series of concentrations of free doxorubicin or M-Dox for 48 hours, and the viability of cells was measured using the methylthiazoletetrazolium method, as previously described (15), Briefly, 100 μL methylthiazoletetrazolium solution (0.5mg/mL in phosphate-buffered saline [PBS]) was added to each well. The plates were incubated for 4 hours at 37 °C. After the incubation, 100 μL dimethyl sulfoxide (Sigma) was added to each well for 10 minutes at room temperature. Absorbance was measured at 570 nm using a plate reader (Thermo, Erlangen, Germany). The mean percentage of cell survival relative to that of untreated cells and 95% confidence intervals (CIs) were estimated from data from three individual experiments. The concentration of doxorubicin at which cell killing was 50% was calculated by curve fitting using SPSS software (version 12.0, SPSS Inc, Chicago, IL).

Quantification of Doxorubicin Internalization

To measure the internalization of doxorubicin quantitatively, A549 cells were cultured on 6-well plates for 24 hours to achieve approximately 80% confluence. M-Dox, free doxorubicin, and empty micelles (doxorubicin concentration, if present, 1 μM; PEG-PE concentration: 2.5 μM) were then added to designated wells. After incubation for specific times, the cells were collected for measurement of doxorubicin fluorescence. To investigate the endocytotic mechanisms that were responsible for internalization of M-Dox, cells were incubated for 30 minutes with either 10 μM filipin (an inhihitor of caveolae-mediated endocytosis), 3 μM cytochalasin D (to inhibit macropinocytosis), 10 μM nystatin (to deplete plasma membrane cholesterol), or 10 μM nocodazole (to inhibit microtubule-mediated endocytosis), followed by 6 hours of incubation with M-Dox (doxorubicin concentration: 1 μM). All inhibitors were from Sigma. The fluorescence from individual cells was detected with a flow cytometer (FACSCalibur, BD, San Jose, CA). For detection of doxorubicin-derived fluorescence, excitation was with the 488-nm line of an argon laser, and emission fluorescence between 564 and 606 nm was measured. For all experiments in which the intracellular doxorubicin was quantified using flow cytomentry, at least 10 000 cells were measured from each sample.

Observation of Endocytosis

To observe endocytosis, A549 cells were cultured on a coverslip in a culture dish (kindly provided by MatTek Corporation, Ashland, MA). The fluorescence from doxorubicin was examined using a total internal reflection fluorescence microscope (TIRFM) system after 10 minutes incubation with M-Dox (17.2 μM) or free doxorubicin (17.2 μM). The TIRFM setup and the lens configuration were described previously (16); briefly, a condenser coupling multiple lasers was attached to the back port of an IX81-inverted automatic microscope (Olympus, Japan) equipped with a ×100 objective lens (numerical aperture = 1.45, Zeiss, Oberkochen, Germany). The 488-nm laser line was used as the excitation wavelength. An appropriate dichroic mirror (DC 488 nm) and emission filter (Long Pass 590 nm) were placed in the light path. We calculated the penetration depth of the evanescent field (d = 138 nm) by measuring the incidence angle using a prism (n = 1.5218) with a 488-nm laser beam. The data were analyzed using the software TILLvisION (TILL Photonics GmbH, Munich BioRegio, Germany).

Subcellular Localization of Doxorubicin

A549 cells were cultured in drug-containing RPMI 1640 medium (1 μM M-Dox, 1 μM free doxorubicin, or 2.5 μM PEG-PE for empty rhodamine-labeled micelles) on 14-mm^2 glass coverslips that were placed in culture dishes (kindly provided by MatTek Corporation) for 12 hours followed by treatment with organelle-selective dyes (from Molecular Probes, Eugene, OR). Cells were incubated with 50 nM LysoTracker Green DND-26 (5 minutes), 40 nM MitoTracker Green FM (30 minutes), and 10 μM Hoechst 333342 (30 minutes) to visualize lysosomes, mitochondria, and nuclei, respectively. The excitation/emission wavelengths were 488 nm/510 nm for LysoTracker and MitoTracker, 340 nm/460 nm for Hoechst 33342, and 488 nm/560 nm for doxorubicin. Cells were treated with 1 μM M-Dox or free doxorubicin in the presence or absence of 20 μM chloroquine for various times, and the subcellular localization of doxorubicin fluorescence was determined using confocal microscopy.

In Vivo Tumor Studies

C57Bl/6 female mice (6–8 weeks old) were from the Institute of Materia Medica, Chinese Academy of Medical Sciences. All animal procedures were performed following the protocol approved by the Institutional Animal Care and Use Committee at the Institute of Biophysics, Chinese Academy of Sciences.

The total number of mice used for the Lewis Lung Carcinoma (LLC) subcutaneous model was 160. The mice were injected subcutaneously in the right flank with 0.2 mL of cell suspension containing 5×10^5 LLC cells (purchased from ATCC) and maintained in DMEM medium. Solid tumor tissue was processed by mechanical and enzymatic (dispase/collagenase deoxyribonuclease) digestion to generate single-cell suspensions. Tumors were allowed to grow for approximately 5 days to a volume of 100–200 mm^3 measured using calipers before treatment. Tumor-bearing mice were randomly assigned to one of the following eight treatment groups (n = 20 mice per group): PEG-PE micelles only (165 mg/kg, single dose), free doxorubicin (5 mg/kg, single dose), M-Dox (5 mg/kg, single dose), M-Dox (15 mg/kg, single dose), PEG-PE micelles only (165 mg/kg each, two doses), free doxorubicin (5 mg/kg each, two doses), M-Dox (5 mg/kg each, two doses), M-Dox (15 mg/kg each, two doses). In single-dose experiments, 80 mice received a single dose on day 5; in the two-dose experiments, 80 mice received doses on day 5 and day 12. Treatments were administered through tail vein injection, and all drugs were diluted with 0.9% sodium chloride. For the tumor growth study, T/C, the ratio of the mean tumor volume in the treated mice (T) divided by that of the control group (C), was determined on day 18. After day 18, control and free doxorubicin–treated mice began to die. For the life span study, the experiment was ended on day 45.

For each treatment group, 10 mice were used for daily monitoring of weight loss and tumor progression (by measurement with calipers). On day 18, these mice were killed by cervical vertebra dislocation, and their tumors and hearts were immediately harvested, weighed, and analyzed. Simultaneously, l mL of blood was drawn by orbital venous puncture for white cell counting. To analyze the cardiac toxicity of treatment regimens to the heart, heart sections were fixed in 10% formalin, dehydrated in incrementally increasing concentrations of alcohol, and stained with hematoxylin and eosin followed by microscopic examination for cardiomyopathy. The remaining 10 mice in each treatment group were used for survival analysis. In the group that received two doses of free doxorubicin, four mice were killed before the endpoint (day 18) because of severe cardiac toxicity.

For the pulmonary metastatic model, 128 mice were injected intravenously through the tail vein with 0.2 mL of a cell suspension containing 5×10^5 LLC cells. The mice were randomly assigned to one of the following eight groups (n = 16 mice per group): PEG-PE micelles only (165 mg/kg, single dose), free doxorubicin (5 mg/kg, single dose), M-Dox (5 mg/kg, single dose), M-Dox (15 mg/kg, single dose), PEG-PE micelles only (165 mg/kg each, three doses), free doxorubicin (5 mg/kg each, three doses), M-Dox (5 mg/kg each, three doses), M-Dox (15 mg/kg each, three doses). In the single-dose experiment, 64 mice received a single dose on

day 10 through tail vein injection. In the three-dose experiment, 64 mice received three doses on day 10, day 17, and day 24 through tail vein injection. All drugs were diluted with 0.9% sodium chloride. For each treatment group, six mice were used to monitor tumor burden in lungs. These mice were killed by cervical vertebra dislocation (on day 24 for the single-dose treatment and on day 31 for the three-dose treatment), and their lungs and hearts were immediately harvested, weighed, and analyzed. The procedure for toxicity analysis described above was used for the subcutaneous tumor model for lung metastatic tumors. The remaining 10 mice in each treatment group were included in the survival analysis.

To study the toxic effects of M-Dox treatment, as indicated by loss of body weight, 30 mice without tumors were randomly assigned to one of three treatment groups (n = 10 mice per group): PEG-PE micelles alone (165 mg/kg each), free doxorubicin (10 mg/kg each), or M-Dox (10 mg/kg each). After tail vein injection, weight was recorded daily. The experiment was ended on day 20.

Detection of Doxorubicin in Tumors

An additional 120 C57B1/6 mice bearing LLC tumors on day 10 after inoculation of 5×10^5 LLC cells (diameter 0.5–1 cm) were randomly assigned to one of three groups (n = 40 mice per group) and injected intravenously through tail vein with M-Dox, free doxorubicin (10 mg/kg for each treatment), or PEG-PE micelles (165 mg/kg) as control. In each treatment group, mice were killed by cervical vertebra dislocation at 6, 12, 24, or 48 hours after drug administration (n = 10 at each time point), and the tumors were excised, weighed, disaggregated by gentle homogenization, resuspended in ice-cold PBS, and filtered through a 50-μm filter. The filtered cells were centrifuged for 10 minutes at 500*g* at 4 °C to remove debris, resuspended in ice-cold PBS (3 mL/g of tumor tissue), and fixed with freshly prepared PBS containing 8% formaldehyde (3 mL/g of tissue). The cells were stored in the dark at 4 °C overnight and then analyzed by flow cytometry for doxorubicin fluorescence as described previously (17). A cell whose fluorescence level exceeded that of 98% of the control cells was defined as fluorescent. For the calculation of population fluorescence intensity, geometric means were determined from flow cytometry data, and the fluorescence value was obtained by subtracting the geometric mean of the control cell population from the geometric mean of the doxorubicin-stained cell population.

Distribution of Micelle-Encapsulated Doxorubicin In Vivo

A total of 72 additional C57Bl/6 mice bearing LLC tumors (diameter 0.5–1 cm) were randomly assigned to two groups (n = 36 mice per group) and injected intravenously through the tail vein with 10 mg/kg of M-Dox or free doxorubicin. In each treatment group, mice were killed by cervical vertebra dislocation at 1, 3, 5, 12, 24, and 48 hours after drug administration (n = 6 at each time point). Serum, tumor, liver, kidney, lung, heart, and spleen were collected, and all the tissues (except serum) were homogenized. Doxorubicin was extracted from all tissues with acidic alcohol (0.3 M HCl : EtOH, 3 : 7, vol/vol) and detected with a fluorimeter using excitation and emission wavelengths of 485 and 590 nm, respectively. The data were normalized to the tissue weight. Bioavailability from 0 to 48 hours (AUC_{0-48}) was calculated from the area under the blood concentration versus time curve using the linear trapezoidal rule.

Statistical Analysis

Data were expressed as the means with 95% confidence intervals. Statistical tests were performed with the Student's *t* test, the Wilcoxon signed rank test, or the Mann–Whitney test. When differences were detected, the Wilcoxon signed rank test was used to test for pairwise differences between treatment groups (SPSS software, version 12.0, SPSS Inc) and the Mann–Whitney test was used to determine the difference between independent sample groups (SPSS software, version 12.0, SPSS Inc). Survival was assessed with the Kaplan–Meier method. For all tests, *P* values less than .05 were considered to be statistically significant. All statistical tests were two-sided.

Results

Entrapment and Stability of Doxorubicin in Polyethylene Glycol–Phosphatidylethanolamine Micelles

We incorporated doxorubicin into PEG-PE micelles using a new self-assembly procedure (shown schematically in Fig. 1, A). Unincorporated doxorubicin was removed by centrifugation through a filter with a molecular mass cutoff of 30 kDa. Entrapment efficiency was defined as the weight percentage of doxorubicin incorporated in micelles. At a molar ratio of doxorubicin to PEG-PE of 1 : 2, the micelles had an entrapment efficiency of 99.4%. TEM showed that both the empty micelles and those encapsulating doxorubicin were monodisperse (Fig. 1, B and C). Incorporation of doxorubicin did not measurably perturb either the geometry or the size of PEG-PE micelles; both empty micelles and those incorporating doxorubicin were spherical with a diameter between 10 and 20 nm (Fig. 1, B and C). These structural characteristics determined by TEM were confirmed in a separate study by nuclear magnetic resonance spectroscopy (data not shown). Upon encapsulation in micelles, the anthracene ring of doxorubicin inserted between the PE phospholipids with the amino sugar of doxorubicin located in the outer shell of the micelle, between the PEG chains (Fig. 1, A; structural characterization of the M-Dox will be reported elsewhere).

The degraded products of doxorubicin incorporated in micelles were detected using HPLC after defined periods of storage. Less than 5% of encapsulated doxorubicin was degraded in pH 7.4 HBS at 4 °C after 6 months; 52% of the free drug was degraded under similar conditions. PEG-PE micelles encapsulating doxorubicin also demonstrated high integrity after storage for 6 months at 4 °C as determined by TEM (Fig. 1, D) while the most of empty micelles did not possess structural integrity after the same storage (data not shown). Thus, encapsulation of doxorubicin in micelles stabilized both doxorubicin and micelles. We were unable to encapsulate doxorubicin to form core-shell nanoparticles with PE alone, suggesting that doxorubicin encapsulation depends on the molecular properties of the PEG-PE diblock copolymer.

Released doxorubicin was separated from micelles by dialysis and quantified fluorimetrically using HPLC. Drug release from M-Dox was much slower at pH 7.0 than at pH 5.0 (Fig. 1, E). Substituting serum isolated from mice for buffer had only a slight effect on the time course of drug release. After 48 hours of incubation at pH 7.0, approximately 24% of total drug was released in the presence of serum compared with the 18% released in the absence of serum (data not shown).

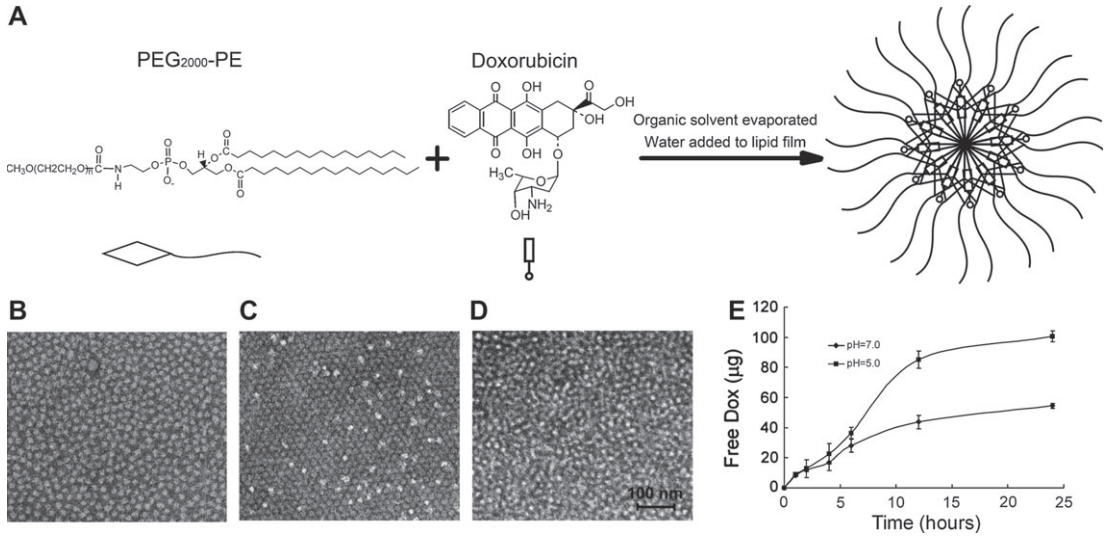

Fig. 1. Nanoassembly of doxorubicin and polyethylene glycol–phosphatidylethanolamine (PEG-PE) and characterization of micelle-encapsulated doxorubicin (M-Dox). **A**) Schematic illustration of self-assembly of doxorubicin and PEG-PE. Both PEG-PE and doxorubicin are amphiphilic. Upon encapsulation in micelles, the hydrophobic anthracene ring of doxorubicin inserted between the PE phospholipids, with the hydrophilic amino sugar of doxorubicin in the outer shell of the micelle between PEG chains. **B**) Transmission electron microscopy (TEM) image of empty PEG-PE micelles stained with 1% uranyl acetate and examined by electron microscopy. **C**) TEM image of M-Dox. **D**) TEM image of micelles incorporating doxorubicin after storage for 6 months at 4 °C. **Scale bar** = 100 nm. **E**) Time course of doxorubicin release from micelles at 37 °C at pH 5.0 or pH 7.0. Released doxorubicin was separated from M-Dox by dialysis and quantified fluorimetrically using HPLC.

Cellular Entry and Cytotoxicity of Micelle-Encapsulated Doxorubicin

We sought to determine whether encapsulation of doxorubicin in micelles would increase drug entry into tumor cells and cytotoxicity. Free doxorubicin or M-Dox in micelles was added to cells cultured on 6-well plates such that doxorubicin concentration was 1 μM, and after incubation for specific times, the cells were collected for analysis of doxorubicin-derived fluorescence by flow cytometry. Doxorubicin incorporated into micelles was more rapidly internalized than free doxorubicin (Fig. 2, A). When cells were incubated with 1 μM M-Dox at 4 °C for 6 hours, the cellular fluorescence intensity was much lower than that in the cells incubated at 37 °C (Fig. 2, B).

To compare cytotoxic activity of encapsulated and free drug, A549 cells were exposed to a series of equivalent concentrations of free doxorubicin or doxorubicin encapsulated in micelles for 48 hours, and the percentage of viable cells was quantified using the methylthiazoletetrazolium method. The concentration of doxorubicin in micelles that caused 50% killing was much lower than that of free doxorubicin (mean = 0.228 versus 0.625 μM, difference = 0.397 μM, 95% CI = 0.274 to 517.6 μM, $P = .001$, Wilcoxon signed rank test) (Fig. 2, C). These results indicate that the encapsulation of doxorubicin in PEG-PE plays an important role in the enhancement of cytotoxic activity. Cytotoxic assays using different exposure times (24–72 hours) yielded similar enhancement of cell killing (data not shown).

To investigate the mechanism of drug entry into cells, we added M-Dox, free doxorubicin, or micelles composed of PEG-PE and labeled with rhodamine-PE to A549 cells and monitored internalization by cells using fluorescence microscopy to detect

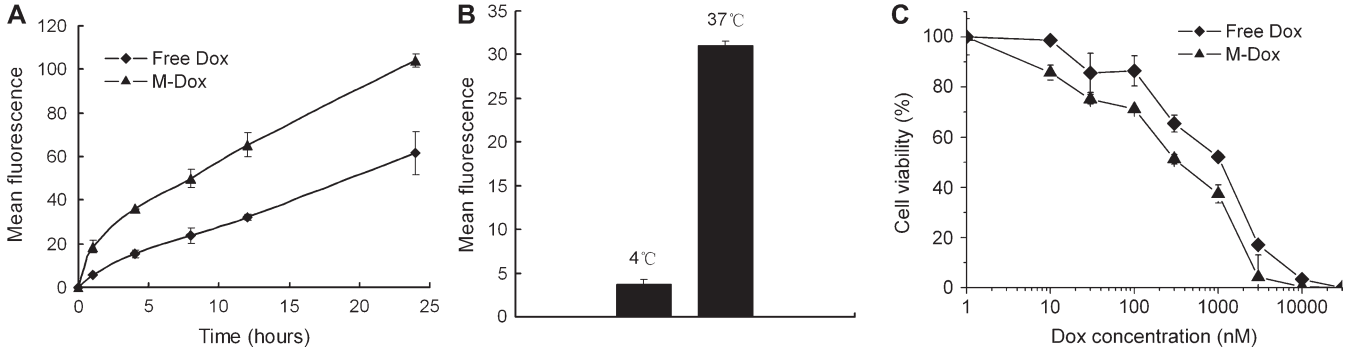

Fig. 2. Cellular uptake and cytotoxic effect of free doxorubicin and micelle-encapsulated doxorubicin (M-Dox) in A549 cells. **A**) Time course of doxorubicin accumulation in cells exposed to 1 μM free doxorubicin (Free Dox, **filled diamonds**) or equivalent concentration of drug encapsulated in micelles (**filled triangles**) as measured by fluorescence. **Error bars** correspond to 95% confidence intervals from three independent experiments. **B**) Internal doxorubicin fluorescence in cells after 6 hours of exposure to 1 μM M-Dox at 4 °C or 37 °C; 95% confidence intervals are shown. **C**) Killing of A549 cells exposed to free doxorubicin (**filled diamonds**) or M-Dox (**filled triangles**) doses ranging from 1 to 10 000 nM for 48 hours. The percentage of viable cells was quantified using the methylthiazoletetrazolium method. Mean values and 95% confidence intervals derived from three independent experiments are shown.

doxorubicin or rhodamine-PE fluorescence. Both M-Dox and free doxorubicin were detectable inside cells (Fig. 3, A–D), whereas no fluorescence was observed in the cells treated with rhodamine-PE–labeled PEG-PE micelles (data not shown). The latter result suggested that the tendency of M-Dox to enter cells was not due to the PEG-PE micelle per se. Instead, the unique structure and properties of the doxorubicin-containing PEG-PE micelle may facilitate the entry of both doxorubicin and PEG-PE.

Next, we addressed whether the cellular uptake of M-Dox occurred through a specific endocytotic pathway. We used TIRFM to monitor internalization of M-Dox by A549 cells. When cells were treated with 17.2 μM M-Dox, the appearance, movement, and disappearance of small vesicles with red fluorescence indicating the presence of doxorubicin was observed within 10 minutes (data not shown). The sizes of the vesicles ranged from 200 to 500 nm. However, no vesicles with red fluorescence could be observed when cells were treated with free doxorubicin, even after longer times.

We tested whether specific endocytotic inhibitors could inhibit the internalization of M-Dox. In these experiments, rhodamine-labeled 70-kDa dextran, a substrate for lipid raft/caveolae-mediated endocytosis (18), was used as a positive control. Among the inhibitors tested, we also included nystatin, which depletes cholesterol from the plasma membrane because cholesterol removal disrupts several lipid raft–mediated endocytotic pathways (19–23). Cells were treated with inhibitors for 30 minutes prior to 6 hours of exposure to M-Dox such that the doxorubicin concentration was 1 μM. Inhibitory effects on M-Dox uptake were not observed in cells treated with 10 μM filipin (an inhibitor of caveolae-mediated endocytosis), 3 μM cytochalasin D (to inhibit macropinocytosis), 10 μM nocodazole (to inhibit microtubule-mediated endocytosis), or 10 μM nystatin. However, treatment of cells with filipin, nystatin, cytochalasin D, and nocodazole did inhibit dextran uptake by approximately 63%, 50%, 43%, and 30%, respectively (data not shown). These results suggest that macropinocytosis, caveolae-mediated endocytosis, and microtubule-mediated pathways are not involved in the uptake of M-Dox.

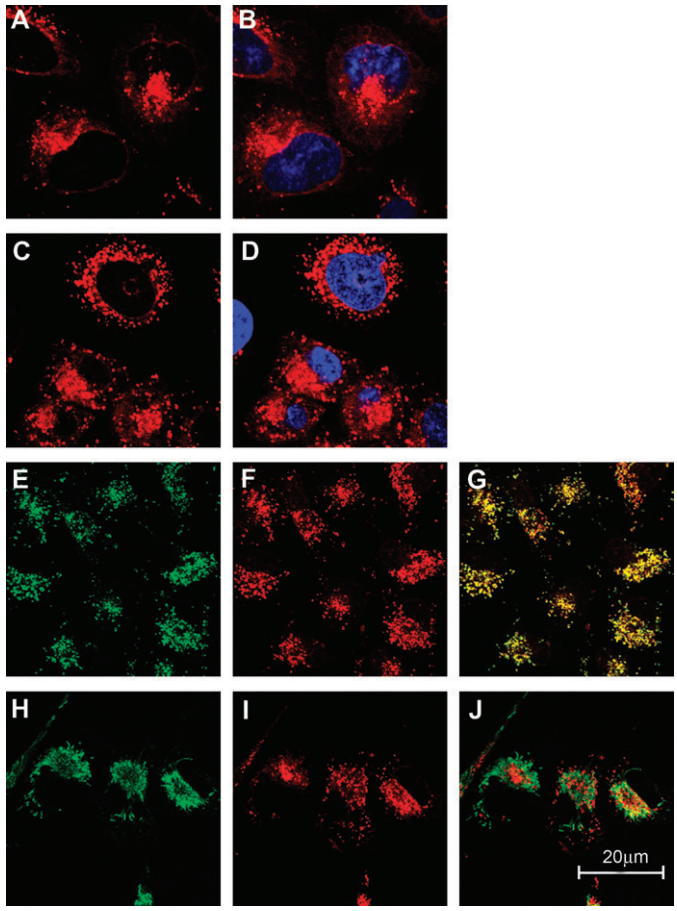

Fig. 3. Localization and distribution of micelle-encapsulated doxorubicin (M-Dox) in A549 cells. Cells were cultured in drug-containing medium (1 μM M-Dox or free doxorubicin) on 14 mm^2 glass coverslips for 12 hours followed by treatment with organelle-selective dyes for 5–30 minutes and subsequent examination by confocal microscopy. **A** and **C**) Confocal images of cells treated with M-Dox or free doxorubicin showing distribution of doxorubicin-derived fluorescence (**red**). **B** and **D**) Overlaid images with **A** and **C** showing nuclear staining using Hoechst 33342 (**blue**). **E** and **F**) Distribution of lysosomes (**green**) in cells labeled with LysoTracker Green (**E**) in cells treated with micelle-encapsulated doxorubicin compared with localization of doxorubicin (**F**). **G**) An overlay of **E** and **F** showing almost a complete colocalization of LysoTracker and doxorubicin-derived fluorescence. **H** and **I**) Distribution of mitochondria (**green**) labeled with MitoTracker green (**H**) in cells treated with M-Dox compared with localization of doxorubicin (**I, red**). **J**) An overlay of **H** and **I** showing little locolization of doxorubicin in mitochondria. **Scale bar** = 20 μm.

Intracellular Distribution of Micelle-Encapsulated Doxorubicin

Confocal microscopy was used to observe the intracellular distribution of internalized doxorubicin. After 12 hours of incubation of A549 cells with M-Dox, fluorescence was localized mainly in specific areas of the cell (Fig. 3, A and B); similar incubation with free doxorubicin resulted in a much more dispersed distribution of fluorescence (Fig. 3, C and D). To determine the cellular distribution more precisely, we performed double fluorescence–labeling experiments and visualized red fluorescence from doxorubicin and green fluorescence from LysoTracker Green DND-26 or MitoTracker Green FM, dyes that are selective for acidic lysosomes (or endosomes) and mitochondria, respectively. Cells were incubated with these dyes for a short period of time after doxorubicin uptake. After M-Dox treatment, most of the doxorubicin was localized to lysosomes, as evidenced by colocalization of red fluorescence with that from LysoTracker Green (Fig. 3, E–G). Colocalization of green and red fluorescence was not observed when cells were labeled with MitoTracker Green (Fig. 3, H–J), indicating that doxorubicin was not specific for mitochondria. To further confirm the lysosomal localization of M-Dox, we treated cells with M-Dox in combination with chloroquine, an ion-transporting ATPase inhibitor that disrupts lysosomes by elevating their pH (24). After 12 hours of incubation of cells with M-Dox in the presence of chloroquine (20 μM) at 37 °C, fluorescence from doxorubicin was localized in large, round compartments (data not shown). After 24 hours, these large, round compartments had disappeared, indicating that doxorubicin assembled in the PEG-PE micelle localized to lysosomes.

Antitumor Effect of Micelle-Encapsulated Doxorubicin in the Lewis Lung Carcinoma Subcutaneous Model

We compared the antitumor effect of M-Dox with that of free doxorubicin in the LLC subcutaneous model. Eighty female

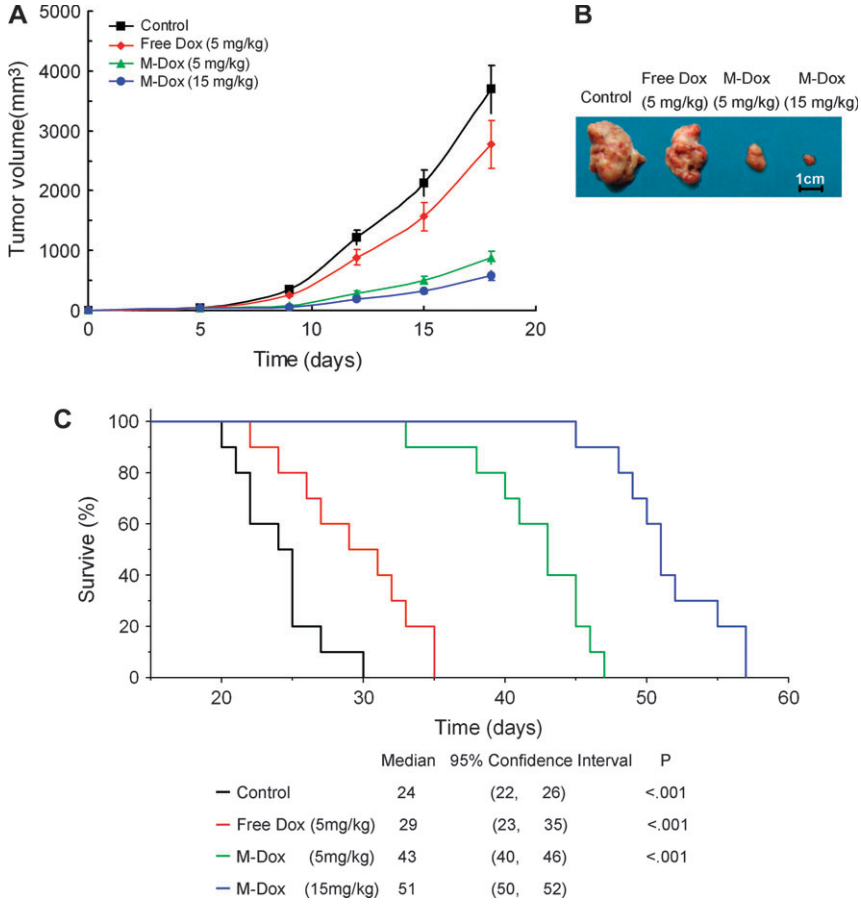

Fig. 4. Antitumor effect of the micelle-encapsulated doxorubicin (M-Dox) in Lewis lung carcinoma (LLC) subcutaneous model. **A**) Mice (n = 10 in each treatment group) were injected subcutaneously with LLC cells. At day 5 and day 12, mice received 5 mg/kg free doxorubicin (Free Dox, **filled diamonds**), 5 mg/kg M-Dox (**filled triangles**), 15 mg/kg M-Dox (**filled circles**), or 165 mg/kg empty polyethylene glycol–phosphatidylethanolamine (PEG-PE) micelles (**filled squares**). Mean values of tumor volumes on days 5, 9, 12, 15, and 18 after injection of carcinoma cells are shown; error bars correspond to 95% confidence intervals. **B**) Photographs of a tumor from each treatment group excised on day 18. **C**) Kaplan–Meier curves showing survival of mice treated with empty PEG-PE micelles (**black**), free 5 mg/kg doxorubicin (**red**), 5 mg/kg M-Dox (**green**), and 15 mg/kg M-Dox **(blue)**. *P* values were from the Mann–Whitney test.

C57Bl/6 mice were inoculated subcutaneously with 5×10^5 LLC cells. On day 5, the mice (20 in each treatment group, 10 for the tumor growth study and 10 for survival analysis) were injected intravenously with 5 mg/kg free doxorubicin, 5 mg/kg doxorubicin in micelles, or 15 mg/kg of doxorubicin in micelles. Mice treated with empty micelles (165 mg/kg) comprised the control group. Tumors were measured daily using calipers. On day 18, T/C was 0.82 (mean = 3021 versus 3693 mm^3, difference = 672 mm^3, 95% CI = 296 to 1049 mm^3, $P = .0332$, Wilcoxon signed rank test) in mice treated with free doxorubicin, 0.31 (mean = 1126 versus 3693 mm^3, difference = 2567 mm^3, 95% CI = 2190 to 2943 mm^3, $P<.001$) in mice treated with 5 mg/kg M-Dox, and 0.20 (mean = 728 versus 3693 mm^3, difference = 2965 mm^3, 95% CI = 2583.3 to 3348.3 mm^3, $P<.001$) in mice treated with 15 mg/kg M-Dox. Thus, tumor growth rates in mice treated with M-Dox were dramatically decreased, whereas free doxorubicin treatment only slightly reduced the tumor growth. Furthermore, there was a substantial increase in the life span of the M-Dox–treated mice; 50% of the mice treated with M-Dox (5 mg/kg) survived 40 days or longer and 90% of the mice treated with M-Dox (15 mg/kg) survived 40 days or longer. By comparison, all mice treated with free doxorubicin and all untreated mice died within 30 days (data not shown). On day 18, we did not observe weight loss in the M-Dox–treated mice, even at the high dose of 15 mg/kg, whereas treatment with 5 mg/kg free doxorubicin was associated with weight loss indicating toxicity (data not shown).

We also examined the effect of treatment with two doses of M-Dox in subcutaneous LLC tumor–bearing mice. Eighty female C57Bl/6 mice were inoculated subcutaneously with 5×10^5 LLC cells. On days 5 and 12, the mice (20 in each treatment group, 10 for tumor growth study and 10 for survival analysis) were injected intravenously with 5 mg/kg free doxorubicin or 5 mg/kg or 15 mg/kg doxorubicin encapsulated in micelles. Control mice were treated with empty micelles (165 mg/kg). Tumors were measured in treated and untreated mice at days 5, 8, 12, 15, and 18 (Fig. 4, A). T/C values on day 18 for treatment with 5 mg/kg free doxorubicin and 5 mg/kg and 15 mg/kg micelle-encapslulated doxorubicin were 0.75, 0.24, and 0.16, respectively. Thus, two separate doses of M-Dox repressed tumor growth to a slightly greater extent than a single dose. Tumors were excised from a mouse from each of the four treatment groups to verify tumor measurements (Fig. 4, B). Four of 10 mice treated with free doxorubicin were euthanized due to cardiac toxicity in tumor growth study. However, mice receiving two doses of M-Dox at 15 mg/kg showed only slight weight loss, indicating that the maximum tolerated dose was not reached. In these experiments, the life span of mice that were treated with 15 mg/kg M-Dox was 51 days (95% CI = 50 to 52 days) compared with 43 days (95% CI = 40 to 46 days) for mice treated with 5 mg/kg M-Dox, 29 days (95% CI = 23 to 35 days) for mice treated with doxorubicin alone, and 24 days (95% CI = 22 to 26 days) in the control group. The life span was statistically significantly longer for the group that received M-Dox at 15 mg/kg with two doses than for all other groups (versus control, $P<.001$;

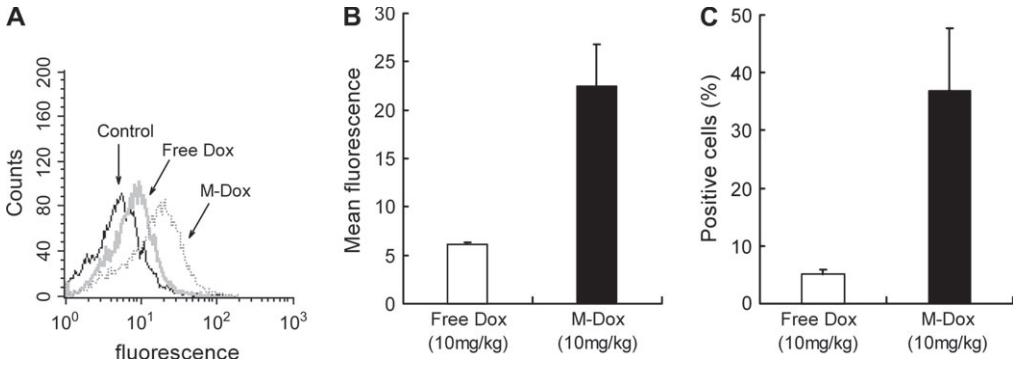

Fig. 5. Penetration of the micelle-encapsulated doxorubicin (M-Dox) in Lewis Lung Carcinoma (LLC) tumors. **A**) Fluorescence-activated cell sorting analysis of cells recovered from LLC tumors 12 hours after in vivo administration of free doxorubicin (Free Dox, 10 mg/kg) and M-Dox (10 mg/kg) or empty polyethylene glycol–phosphatidylethanolamine micelles (165 mg/kg) as control. **B**) The geometric mean of fluorescence intensity of LLC cells recovered from tumors (n = 10 tumors from 10 different mice) when mice were treated with free doxorubicin or M-Dox. **Error bars** correspond to 95% confidence intervals. **C**) The percentage of doxorubicin-containing cells recovered from LLC tumors (n = 10 tumors from 10 different mice). **Error bars** correspond to 95% confidence intervals.

versus free doxorubicin, $P<.001$; versus M-Dox at 5 mg/kg with two doses, $P<.001$, Mann–Whitney test). In the high–double-dose group, no death was observed during this study, which ended on day 45 (Fig. 4, C)

Penetration of Micelle-Encapsulated Doxorubicin in Tumors

To investigate whether encapsulation of the doxorubicin increased its penetration into tumors, we measured the fluorescence of cells from LLC tumors 12 hours after intravenous administration of free doxorubicin or M-Dox. In preliminary experiments, we observed that the fluorescence signal from cells that had been exposed to doxorubicin was stable for at least 24 hours after formaldehyde fixation at 4 °C (data not shown). C57B1/6 mice bearing tumors were injected with free doxorubicin or M-Dox, and tumors were excised, disaggregated after homogenization, and fixed. Flow cytometry of fixed tumor cells was used to quantify penetration of doxorubicin into tumor cells. The distribution of fluorescence intensities in sets of cells from mice exposed to free doxorubicin (10 mg/kg) or M-Dox (10 mg/kg) or empty PEG-PE micelles (165 mg/kg) was shown in Fig. 5, A. Injection of doxorubicin encapsulated in micelles increased the mean fluorescence intensity (Fig. 5, B) and the ratio of fluorescence-positive cells (Fig. 5, C) recovered from LLC tumors 12 hours after injection by 3.7 fold (mean = 22.52 versus 6.14 arbitrary units, difference = 16.38, 95% CI = 5.95 to 26.81, $P = .021$) and 7.2 fold (mean = 36.9% versus 5.1%, difference = 31.8%, 95% CI = 16.5% to 47.0%, $P = .004$, Student's t test), respectively, compared with free doxorubicin. Thus, encapsulation in micelles increased the penetration of the drug into cells in vivo.

Antitumor Effect of Micelle-Encapsulated Doxorubicin in the Lewis Lung Carcinoma Pulmonary Model

To test whether M-Dox was effective against an established syngeneic lung metastasis, we injected LLC cells intravenously into 64 C57Bl/6 mice. To ensure that all mice bore actively growing lung tumors before the drug treatment, pulmonary cancer was allowed to develop for 10 days. In a single-dose experiment, after establishment of tumors, the mice (16 in each treatment group, 6 for lung tumor burden study and 10 for survival analysis) were injected intravenously on day 10 with 5 mg/kg free doxorubicin or 5 mg/kg or 15 mg/kg doxorubicin encapsulated in micelles or empty micelles (165 mg/kg). In a separate experiment, three doses of drug at the same concentrations as in the single-dose experiment were administered on days 10, 17, and 24 to 16 mice in each treatment group (6 for the lung tumor burden study and 10 for survival analysis).

At day 24, mice treated with a single dose of M-Dox displayed few or no visible metastases (Fig. 6, A), whereas all mice treated with empty PEG-PE micelles or free doxorubicin had an extensive tumor burden in the lungs (Fig. 6, A and B). The inhibitory effect on metastasis of M-Dox was reflected in a statistically significant reduction in tumor weight in the lung at day 24 compared with control (mean for mice treated with 5 mg/kg M-Dox = 0.12 versus 0.33 g in controls, difference = 0.21 g, 95% CI = 0.15 to 0.26 g, $P<.001$, and mean for mice treated with 15 mg/kg M-Dox = 0.05 versus 0.33 g, difference = 0.28 g, 95% CI = 0.23 to 0.34 g, $P<.001$, Student's t test). Treatment with 5 mg/kg of free doxorubicin did not cause a statistically significant reduction in tumor weight compared with control (mean = 0.34 versus 0.33 g) (Fig. 6, B). When three doses were given, treatment with M-Dox was associated with less tumor burden in the lungs compared with a single dose (data not shown).

We also tested survival and toxicity in mice receiving a single dose or three doses of M-Dox. In the single-dose experiment, mice treated with 15 mg/kg M-Dox had a median life span of 79 days (95% CI = 74 to 84 days) compared with 63 days (95% CI = 60 to 66 days) for mice treated with 5 mg/kg M-Dox, 29 days (95% CI = 24 to 34 days) for mice treated with 5 mg/kg free doxorubicin, and 30 days (95% CI = 21 to 40 days) for the control group (Fig. 6, C). The life span of mice treated with 15 mg/kg M-Dox was statistically significantly longer than that of mice treated with 5 mg/kg M-Dox ($P = .028$), free doxorubicin ($P = .005$), and controls ($P = .005$, Mann–Whitney test). In the experiment in which the drugs were administered in three doses, the median life span of mice treated with 15 mg/kg M-Dox was 91 days (95% CI = 85 to 97 days) compared with 70 days (95% CI = 62 to 78 days) in mice treated with 5 mg/kg M-Dox, 24 days (95% CI = 22 to 26 days) in mice treated with 5 mg/kg free doxorubicin, and 30 days (95% CI = 21 to 40 days) for the control group (Fig. 6, D). The life span of mice treated with 15 mg/mL M-Dox was statistically significantly longer than that of mice treated with 5 mg/kg M-Dox, 5 mg/kg free doxorubicin, and control ($P = .023$, .002, and .005, respectively, Mann–Whitney test).

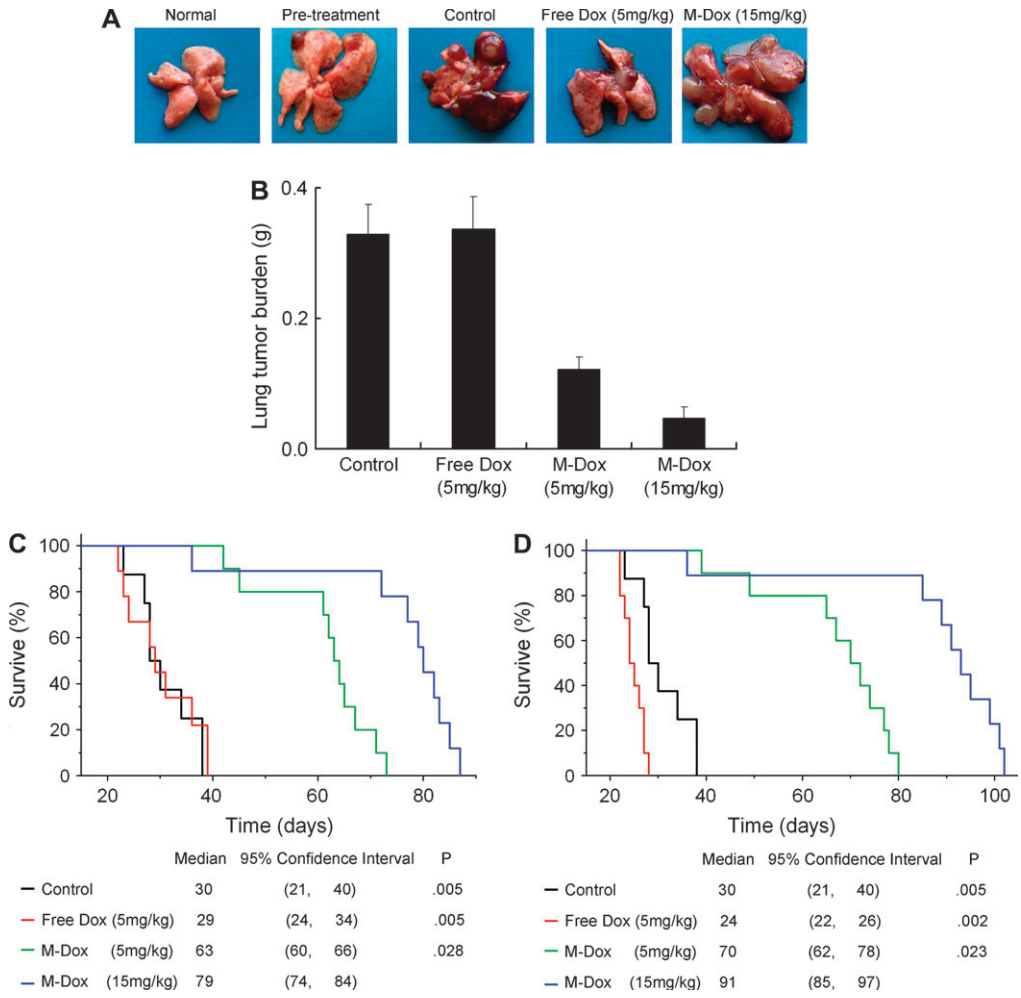

Fig. 6. Antitumor effect of the micelle-encapsulated doxorubicin (M-Dox) in the Lewis lung carcinoma pulmonary model. Mice were injected with free doxorubicin (Free Dox) or M-Dox or empty polyethylene glycol–phosphatidylethanolamine (PEG-PE) micelles as control at day 10 after establishment of tumors. Lungs were harvested at day 24, photographed (**A**), and weighed (**B**); mean values are shown for lung tumor burden in mice treated with free doxorubicin or M-Dox; **error bars** correspond to 95% confidence intervals; n = 6 mice per group). **C** and **D**) Kaplan–Meier graphs showing survival of mice treated with a single dose (**C**) or multiple doses (**D**) of 165 mg/kg empty PEG-PE micelles (**black**), free 5 mg/kg doxorubicin (**red**), 5 mg/kg M-Dox (**green**), or 15 mg/kg M-Dox (**blue**). *P* values were derived from the Mann–Whitney test.

We did not observe death in the high–multiple-dose group for 2 weeks after receiving the final dose. The shorter life span of mice treated with free doxorubicin relative to control mice treated with empty micelles (Fig. 6, D) indicated that free doxorubicin at this doses was highly toxic.

Accumulation and Distribution of Micelle-Encapsulated Doxorubicin in Tumors and Organs

As shown above, encapsulation of doxorubicin in PEG-PE micelles increased the suppression of both tumor growth and metastasis and reduced toxicity. To investigate the basis of the increased effectiveness and reduced toxicity of M-Dox, we determined the pharmacokinetics of doxorubicin both in tumors and in the systemic circulation. For this analysis, we used C57Bl/6 mice bearing LLC tumors that were injected intravenously with free doxorubicin or M-Dox (10 mg/kg) and serum, tumor, liver, kidney, lung, heart, and spleen were collected up to 48 hours after injection, and all the tissues except for serum were homogenized. After its extraction from the tissue-based samples or serum, doxorubicin levels were determined by fluorescence.

Bioavailability, calculated from the area under the blood concentration versus time curve from 0 to 48 hours ($AUC_{0–48}$), was compared for free doxorubicin and M-Dox. The $AUC_{0–48}$ for M-Dox was 10.5 times higher than that for free doxorubicin (mean = 59.5 versus 5.6 μg h/mL, difference = 53.9 μg h/mL, 95% CI = 48.3 to 59.4 μg h/mL, *P*<.001, Wilcoxon signed rank test) (Fig. 7, A). Furthermore, the $AUC_{0–48}$ for M-Dox in tumors was 5.14 times higher than that for free doxorubicin (mean = 201 versus 39 μg h/g, difference = 162 μg h/g, 95% CI = 112 to 213 μg h/g, *P*<.001) (Fig. 7, B). The accumulation in the heart at 12 hours after injection was less than 50% for M-Dox compared with free doxorubicin (mean = 1.9 versus 3.0 μg/g, difference = 1.1 μg/g, 95% CI = 0.1 to 2.2 μg/g, *P* = .039, Wilcoxon signed rank test) (Fig. 7, C). M-Dox accumulation was also higher than that of free doxorubicin in the liver (mean = 12.2 versus 9.8 μg/g, difference = 2.4 μg/g, 95% CI = 0.78 to 5.4 μg/g, *P* = .126), spleen (mean = 24.5 versus 16.8 μg/g, difference = 7.7 μg/g, 95% CI = 0.8 to 14.5 μg/g, *P* = .031), and kidney (mean = 11.7 versus 5.0 μg/g, difference = 6.7 μg/g, 95% CI = 4.5 to 8.4 μg/g, *P*<.01), but in the lung it was somewhat lower (mean = 6.8 versus 9.5 μg/g, difference = 2.7 μg/g, 95% CI = 0.4 to 5.0 μg/g, *P* = .085; Fig. 7, C).

Systemic Toxicity of Micelle-Encapsulated Doxorubicin

Doxorubicin treatment results in severe irreversible cardiomyopathy and reduction of white blood cell (WBC) counts in humans (25). We therefore compared the systemic toxicity of free doxorubicin and M-Dox. Mice without tumors were administered a dose of 10 mg/kg M-Dox or free doxorubicin, or as control 165 mg/kg

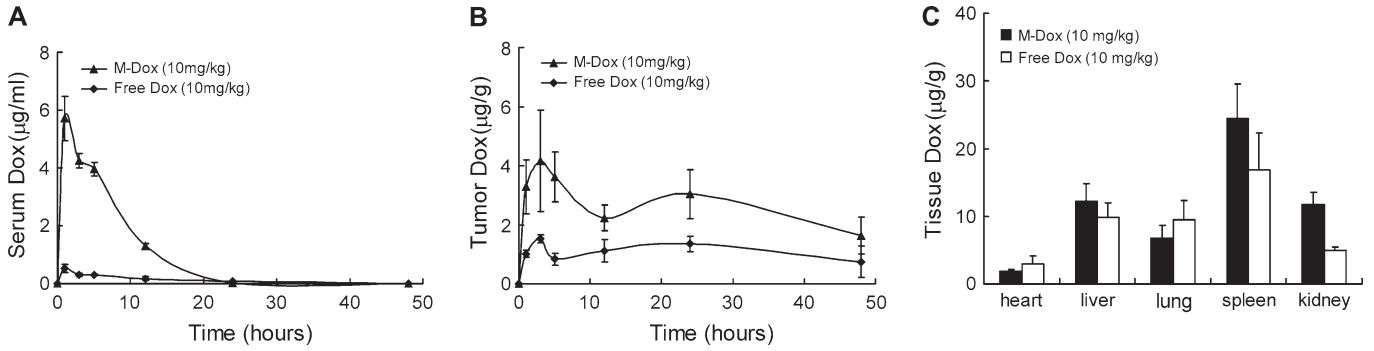

Fig. 7. In vivo distribution and accumulation of micelle-encapsulated doxorubicin (M-Dox) in the Lewis Lung Carcinoma subcutaneous model. Areas under the curves over a period of 48 hours are shown for doxorubicin in serum (**A**) and tumors (**B**) in C57B1/6 mice receiving an intravenous injection of M-Dox (10 mg/kg; **filled triangles**) or free doxorubicin (Free Dox, 10 mg/kg; **filled diamonds**). (**C**) Mean doxorubicin concentrations 12 hours after injection of doxorubicin in heart, liver, lung, spleen, and kidney of mice treated with M-Dox (10 mg/kg; **filled bars**) or free doxorubicin (10 mg/kg; **open bars**); **error bars** correspond to 95% confidence intervals (n = 6 mice per group).

PEG-PE micelles, and body weight was monitored. The mice that were administered free doxorubicin died before the planned endpoint (20 days) after a continuous decrease in body weight. In contrast, mice treated with the same dose of M-Dox began to gain weight within 4–5 days of the start of treatment and attained body weight equal to of that of control on day 11. After killing on day 18, examination of the WBCs showed that treatment with M-Dox (5 mg/kg) was associated with negligible decrease in WBCs (mean = 11.5 versus 12.4 counts/mm^3, difference = 0.9 counts/mm^3, 95% CI = 0.7 to 2.6 counts/mm^3, P = .252, Wilcoxon signed rank test), whereas treatment with free doxorubicin (5 mg/kg) was associated with a statistically significant drop in WBCs (mean = 6.4 versus 12.4 counts/mm^3, difference = 6.0 counts/mm^3, 95% CI = 4.4 to 7.7 counts/mm^3, P<.01), compared with empty PEG-PE micelle group as a normal control. Free doxorubicin also caused severe histopathologic lesions that manifested as myocarditis (data not shown). The muscle fibers showed varying degrees of damage ranging from loss of striation to complete fragmentation (Fig. 8, B). Histopathologic changes in cardiac tissues from mice treated with M-Dox showed only slight signs of toxicity to muscle fibers (Fig. 8, C), compared with the normal muscle fibers from mice receiving empty micelles (Fig. 8, D).

Discussion

To our knowledge, this is the first report of the use of doxorubicin and PEG-PE as a drug delivery system. We demonstrated that the PEG-PE–based nanoparticle containing doxorubicin has several qualities that are necessary in cancer therapy: 1) fast cellular uptake that ensures rapid penetration and enrichment in tumor cells once the M-Dox reaches the tumor site; 2) optimal particle size [i.e., 10–20 nm the size that previously showed maximal accumulation and the deepest penetration into tumors (11)]; 3) a tightly packed structure that allows a longer circulation in plasma (Fig. 7, A) and lack of toxicity to normal organs and tissues due to decreased free drug; and 4) localization that is specific to lysozomes where the drug is released from the nanoassembly to exert its antitumor activity. No fluorescence was observed in the cells treated with

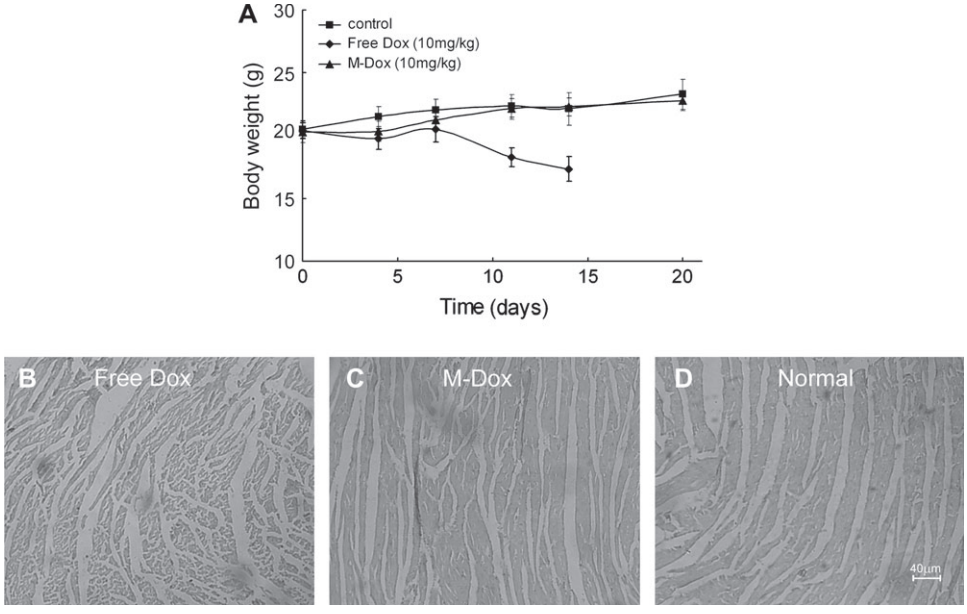

Fig. 8. Systemic toxicity of micelle-encapsulated doxorubicin (M-Dox) in C57B1/6 mice. **A**) Mean body weights at days 0, 4, 7, 11, 14, and 20 of mice treated with single dose of free doxorubicin (Free Dox, 10 mg/kg; **filled diamonds**), M-Dox (10 mg/kg; **filled triangles**), or empty polyethylene glycol–phosphatidylethanolamine (PEG-PE) micelles as control (165 mg/kg; **filled squares**); **error bars** correspond to 95% confidence intervals (n = 10 mice per group). **B**–**D**) Section of cardiac tissue obtained from C57B1/6 mice who had pulmonary metastases from intravenous injection of Lewis Lung Carcinoma cells receiving a single intravenous dose of free doxorubicin (5 mg/kg [**B**]); M-Dox (5 mg/kg [**C**]), or empty PEG-PE micelles (165 mg/kg [**D**]). **Scale bar** = 40 μm. Hearts were harvested at day 24 after intravenous injection.

rhodamine-PE–labeled PEG-PE micelles (data not shown). The latter result suggested that the tendency of M-Dox to enter cells was not due to the PEG-PE micelle per se.

Encapsulation of doxorubicin into PEG-PE micelles increased its accumulation and penetration in tumors in terms of both the percentage of cells that were reached by the drug and the intracellular levels that were attained. This increased accumulation and penetration can be attributed to the efficient internalization of the drug-containing micelles by the endocytotic cell uptake mechanism and enhanced permeability and retention of tumors with leaky vasculature (26). High intracellular retention is especially important because doxorubicin must be internalized to be effective in tumor therapy. The doxorubicin-containing PEG-PE micelles had greatly increased antitumor activity in both subcutaneous and lung metastatic LLC tumor models compared with free doxorubicin (Figs 4 and 6). However, mice treated with M-Dox showed fewer signs of toxicity than those treated with free doxorubicin.

In the past decade, various polymeric micelles have been developed as carriers for antitumor drugs, and there are several reports of clinical use of micelles loaded with drugs such as doxorubicin or taxol (27–29). The greatest challenges encountered in these attempts to use micelles as drug carriers were inadequate stability (30,31) and decreased cytotoxicity against tumor cells compared with the drug alone (27–29,32). Encapsulation of the drugs in polymeric micelles greatly reduced systemic toxicity due to slower release in neutral body fluid. However, because of the decreased cytoxicity, a high dose of drug in the micelles was used in the clinic (29,33). Higher doses in clinical use could result in problems of drug accumulation in other tissues and effects on metabolism. Indeed, such problems have been observed for PEG-modified liposomal doxorubicin (Doxil) (34,35). By contrast, in this study, M-Dox showed stronger antitumor activity both in vitro and in vivo compared with the same dose of free doxorubicin. The differences in effectiveness and toxicities in studies of micelle-encapsulated drugs that have been reported indicate that the choice of nanocarrier is critical and that cancer therapies based on polymeric micelles can provide improved drug efficacy without increasing the chemotherapeutic drug dose while also reducing systemic toxicity.

The most important limitation in the study is the lack of clear mechanistic understanding of how M-Dox works at cellular and molecular levels. Therefore, our results cannot be simply applied to the micellization of other drugs, and there is a need for further investigation in how micellization affects drug uptake and activity.

After 6 months of storage of doxorubicin incorporated in micelles in HBS at pH 7.4 at 4 °C, the degraded products represented less than 5% of the total doxorubicin; however, 52% of the free drug was degraded under similar conditions. PEG-PE micelles encapsulating doxorubicin also demonstrated high integrity as observed by TEM after storage for 6 months at 4 °C (Fig. 1, D) while most of the empty micelles did not possess structural integrity under similar conditions (data not shown). Based on these results, we infer that the stabilities of both PEG-PE micelles and doxorubicin were enhanced in PEG-PE micelles encapsulating doxorubicin. In addition, the entry of doxorubicin in the form of M-Dox was faster than that of free doxorubicin in spite of the fact that cellular uptake of micelles composed of PEG-PE and incorporating rhodamine-PE was not observed (Fig. 3). Furthermore, the doxorubicin that entered cells in the M-Dox form was concentrated in lysosomes, whereas free doxorubicin distribution in cells was much more dispersed. Therefore, the properties of M-Dox are due to the combination of PEG-PE and doxorubicin; they do not derive solely from PEG-PE micelles but from structural determinants of the complex.

In a separate study of of M-Dox using nuclear magnetic resonance spectroscopy (data not shown), PEG-PE and doxorubicin were revealed to be tightly packaged (Fig. 1), possibly due to the amphiphilic nature of the two molecules as well as their specific structures. The physicochemical reasons for the tight packaging can be tested experimentally by chemically modifying PEG-PE and doxorubicin. If molecular fitting, instead of the drug molecule wrapping, proves to be critical to the properties of M-Dox, this may suggest a new structural approach to drug design and micellization.

Our findings as to the effectiveness of M-Dox could have important clinical applications for cancer therapy. The tightly packed structure of M-Dox may be the source of its high antitumor activity and low systemic toxicity, and this property should be considered in the construction of nanoassemblies as delivery systems for other chemotherapeutic molecules.

References

(1) Carmeliet P, Jain RK. Angiogenesis in cancer and other diseases. Nature 2000;407:249–57.

(2) Jain RK, Au P, Tam J, Duda DG, Fukumura D. Engineering vascularized tissue. Nat Biotechnol 2005;23:821–3.

(3) Duda DG, Cohen KS, Kozin SV, Perentes JY, Fukumura D, Scadden DT, et al. Evidence for incorporation of bone marrow-derived endothelial cells into perfused blood vessels in tumors. Blood 2006;107:2774–6.

(4) Jain RK. Normalization of tumor vasculature: an emerging concept in antiangiogenic therapy. Science 2005;307:58–62.

(5) Jain RK. Barriers to drug delivery in solid tumors. Sci Am 1994; 271:58–65.

(6) Jang SH, Wientjes MG, Lu D, Au JL. Drug delivery and transport to solid tumors. Pharm Res 2003;20:1337–50.

(7) Primeau AJ, Rendon A, Hedley D, Lilge L, Tannock IF. The distribution of the anticancer drug doxorubicin in relation to blood vessels in solid tumors. Clin Cancer Res 2005;11:(24 Pt 1):8782–8.

(8) Lankelma J, Dekker H, Luque FR, Luykx S, Hoekman K, van der Valk P, et al. Doxorubicin gradients in human breast cancer. Clin Cancer Res 1999;5:1703–7.

(9) Curnis F, Sacchi A, Corti A. Improving chemotherapeutic drug penetration in tumors by vascular targeting and barrier alteration. J Clin Invest 2002;110:475–82.

(10) Tong RT, Boucher Y, Kozin SV, Winkler F, Hicklin DJ, Jain RK. Vascular normalization by vascular endothelial growth factor receptor 2 blockade induces a pressure gradient across the vasculature and improves drug penetration in tumors. Cancer Res 2004;64:3731–6.

(11) Dreher MR, Liu W, Michelich CR, Dewhirst MW, Yuan F, Chilkoti A. Tumor vascular permeability, accumulation, and penetration of macromolecular drug carriers. J Natl Cancer Inst 2006;98:335–44.

(12) Torchilin VP. Lipid-core micelles for targeted drug delivery. Curr Drug Deliv 2005;2:319–27.

(13) Torchilin VP, Lukyanov AN, Gao Z, Papahadjopoulos-Sternberg B. Immunomicelles: targeted pharmaceutical carriers for poorly soluble drugs. Proc Natl Acad Sci USA 2003;100:6039–44.

(14) Gao Z, Lukyanov AN, Singhal A, Torchilin VP. Diacyllipid-polymer micelles as nanocarriers for poorly soluble anticancer drugs. Nano Lett 2002;2:979–82.

(15) Mosmann T. Rapid colorimetric assay for cellular growth and survival: application to proliferation and cytotoxicity assays. J Immunol Methods 1983;65:55–63.
(16) Xia S, Xu L, Bai L, Xu ZQ, Xu T. Labeling and dynamic imaging of synaptic vesicle-like microvesicles in PC12 cells using TIRFM. Brain Res 2004;997:159–64.
(17) Luk CK, Tannock IF. Flow cytometric analysis of doxorubicin accumulation in cells from human and rodent cell lines. J Natl Cancer Inst 1989;81:55–9.
(18) Huth US, Schubert R, Peschka-Suss R. Investigating the uptake and intracellular fate of pH-sensitive liposomes by flow cytometry and spectral bio-imaging. J Control Release 2006;110:490–504.
(19) Liu NQ, Lossinsky AS, Popik W, Li X, Gujuluva C, Kriederman B, et al. Human immunodeficiency virus type 1 enters brain microvascular endothelia by macropinocytosis dependent on lipid rafts and the mitogen-activated protein kinase signaling pathway. J Virol 2002;76: 6689–700.
(20) Nichols BJ, Lippincott-Schwartz J. Endocytosis without clathrin coats. Trends Cell Biol 2001;11:406–12.
(21) Parton RG, Joggerst B, Simons K. Regulated internalization of caveolae. J Cell Biol 1994;127:1199–215.
(22) Pelkmans L, Helenius A. Endocytosis via caveolae. Traffic 2002; 3:311–20.
(23) Barratt GM. Therapeutic applications of colloidal drug carriers. Pharm Sci Technolo Today 2000;3:163–71.
(24) Seglen PO, Grinde B, Solheim AE. Inhibition of the lysosomal pathway of protein degradation in isolated rat hepatocytes by ammonia, methylamine, chloroquine and leupeptin. Eur J Biochem 1979;95:215–25.
(25) Olson RD, Mushlin PS. Doxorubicin cardiotoxicity: analysis of prevailing hypotheses. FASEB J 1990;4:3076–86.
(26) Maeda H, Wu J, Sawa T, Matsumura Y, Hori K. Tumor vascular permeability and the EPR effect in macromolecular therapeutics: a review. J Control Release 2000;65:271–84.
(27) Matsumura Y, Hamaguchi T, Ura T, Muro K, Yamada Y, Shimada Y, et al. Phase I clinical trial and pharmacokinetic evaluation of NK911, a micelle-encapsulated doxorubicin. Br J Cancer 2004;91:1775–81.
(28) Hamaguchi T, Matsumura Y, Suzuki M, Shimizu K, Goda R, Nakamura I, et al. NK105, a paclitaxel-incorporating micellar nanoparticle formulation, can extend in vivo antitumour activity and reduce the neurotoxicity of paclitaxel. Br J Cancer 2005;92:1240–6.
(29) Kim TY, Kim DW, Chung JY, Shin SG, Kim SC, Heo DS, et al. Phase I and pharmacokinetic study of Genexol-PM, a cremophor-free, polymeric micelle-formulated paclitaxel, in patients with advanced malignancies. Clin Cancer Res 2004;10:3708–16.
(30) Toncheva V, Schacht E, Ng SY, Barr J, Heller J. Use of block copolymers of poly (ortho esters) and poly (ethylene glycol) micellar carriers as potential tumour targeting systems. J Drug Target 2003;11: 345–53.
(31) Liu J, Zeng F, Allen C. Influence of serum protein on polycarbonate-based copolymer micelles as a delivery system for a hydrophobic anticancer agent. J Control Release 2005;103:481–97.
(32) Nishiyama N, Okazaki S, Cabral H, Miyamoto M, Kato Y, Sugiyama Y, et al. Novel cisplatin-incorporated polymeric micelles can eradicate solid tumors in mice. Cancer Res 2003;63:8977–83.
(33) Nakanishi K, Fukushima S, Okamoto K, Suzuki M, Matsumura Y, Yokoyama M, et al. Development of the polymer micelle carrier system for doxorubicin. J Control Release 2001;74:295–302.
(34) Uziely B, Jeffers S, Isacson R, Kutsch K, Wei-Tsao D, Yehoshua Z, et al. Liposomal doxorubicin: antitumor activity and unique toxicities during two complementary phase I studies. J Clin Oncol 1995;13: 1777–85.
(35) Ranson MR, Carmichael J, O'Byrne K, Stewart S, Smith D, Howell A. Treatment of advanced breast cancer with sterically stabilized liposomal doxorubicin: results of a multicenter phase II trial. J Clin Oncol 1997; 15:3185–91.

Funding

Supported by grants from State Key Development Plan Project (2006CB705706 and 2006CB933305), National Natural Science Foundation of China (30470373, 30530180, and 90606019), and the Chinese Academy of Sciences (KSCX2-YW-R-21 and KJCX2-YW-M02). The study sponsors had no role in the design of the study; the collection, analysis, and interpretation of the data; the writing of the manuscript; or the decision to submit the manuscript for publication.

Funding to pay the Open Access publication charges for this article was provided by the National Natural Science Foundation of China (90606019).

Notes

N. Tang and G. Du contributed equally to this work.

The authors thank Dr Sarah Perrett for editing the manuscript and Dr Chunling Zhang, Dandan Yi, and Zhenwei Yang for technical assistance and scientific discussion.

Manuscript received November 8, 2006; revised May 2, 2007; accepted May 23, 2007.